The Effect of Ischaemic Region Shape on ST Potentials using a Half-Ellipsoid Model of the Left Ventricle

JP Barnes, PR Johnston

Griffith University, Brisbane, Australia

Abstract

Extracellular epicardial potential distributions (EPDs) were obtained using a half-ellipsoidal model of the left ventricle for three separate ischaemic geometries (rectangular, cylindrical and semi-ellipsoidal). The transient bidomain equations were numerically solved using a finite volume method for the spatial discretisation and a semi-implicit method for the time integration. Anisotropic conductivities, based on measured values, along with linear fibre rotation, were used throughout the myocardium. Ischaemia was included by taking into account three of the main physiological cellular consequences, including hyperkalaemia, acidosis and anoxia.

Results showed that, at low thicknesses of ischaemia (<40%), a single depression was found on the EPDs for all ischaemic geometries, located above the border of the ischaemic region. As the ischaemic thickness was increased beyond 40%, areas of elevation and depression were apparent on the epicardium for rectangular and cylindrical ischaemic geometries. Elevation was not noticed for the ellipsoidal ischaemic geometry until the ischaemic thickness reached 50%. As the ischaemia became transmural, the EPDs for all three ischaemic geometries were quite similar, with an area of elevation located directly over the ischaemic region, surrounded by depression.

1. Introduction

Subendocardial ischaemia is widely thought of as the cause for ST segment depression in the electrocardiogram (ECG) [1]. Many numerical [2–4] and experimental [5, 6] studies have been conducted in order to understand the mechanisms behind this behaviour. The results from these studies agree quite well for transmural ischaemia, where the ischaemic region extends to the epicardium. When the ischaemia is only partial thickness, however, the results begin to vary. This is partly due to differing choices in vital model parameters, such as tissue conductivity and fibre orientation. One interesting result from these numerical studies was the formation of current loops around the ischaemic border zone, which arise as the result of 'injury currents' between tissue of differing transmembrane potential.

Recently, it was proposed that the shape of the ischaemic geometry affected the formation of these current loops [7, 8]. These studies used a simple slab model to represent a ventricular wall along with three different ischaemic geometries (rectangular, cylindrical and semi-ellipsoidal), which represented a decrease in the presence of 'sharp edges'. The first of the two studies solved the steady state bidomain equations using an artificial transmembrane potential, while the second solved the full transient bidomain equations using a realistic model of cardiac cells.

Results from these two studies showed that at low ischaemic thicknesses (<30%), a single depression was located above the centre of the ischaemic region. As the ischaemic thickness increased, the single depression separated into three distinct depressions for the rectangular and cylindrical ischaemic geometries, one centred over the ischaemic region, and two over opposing lateral borders. For the ellipsoidal ischaemic geometry, however, the central depression was not apparent for medium thicknesses of ischaemia. Elevation in the ST potentials, for all three ischaemic geometries, did not occur until the ischaemic thickness reached 70%.

The motivation for the present study is to investigate whether the results obtained for the simple slab model were also valid using a more realistic, semi-ellipsoidal model of the left ventricle. The transient bidomain equations were solved using a realistic cell model, which incorporated the three major physiological consequences of ischaemia.

2. Methods

Similarly to [8], the bidomain equations [9] were used to calculate the extracellular potentials of the cardiac tissue.

$$\nabla \cdot (M_i + M_e)\nabla\phi_e = -\nabla \cdot M_i \nabla\phi_m, \quad (1)$$

$$\nabla \cdot M_i \nabla\phi_m + \nabla \cdot M_i \nabla\phi_e = \beta \left[C_m \frac{\partial \phi_m}{\partial t} + i_{ion} \right], \quad (2)$$

where ϕ_m and ϕ_e are the transmembrane and extracellular potentials, M_i and M_e are the intracellular and extracellular conductivity tensors of the tissue, C_m is the cell membrane capacitance, β is the cell surface area to volume ratio and i_{ion} represents a collection of ionic processes which make up the cell model. Equation (1) is the steady state bidomain equation and equation (2) [10] describes the transient behaviour. A blood bath was also included which was positioned in contact with the endocardial surface. The governing equation used for the potential in the blood was

$$\nabla^2 \phi_b = 0. \tag{3}$$

The ventricular model used was based on the mesh described in [3]. It was constructed by taking the top half of an ellipsoid which was represented by the parametric equations

$$x = a\cos(\theta)\cos(\phi), \tag{4}$$
$$y = b\cos(\theta)\sin(\phi), \tag{5}$$
$$z = c\sin(\theta), \tag{6}$$

where $-\pi \leq \phi \leq \pi$ and $0 \leq \theta \leq \frac{\pi}{2}$. For the values of a, b and c, the endocardial surface used $a = 2$, $b = 2$ and $c = 4$, while the epicardial surface used $a = 3$, $b = 3$ and $c = 5$. This gave a uniform tissue thickness of 1 cm for the entire model. The model included anisotropic conductivities, based on the experiments by Clerc [11], and also included a total fibre rotation from the endocardium to the epicardium of 120°. The model included a total of 1,003,721 nodes in the tissue and 356,445 nodes in the blood.

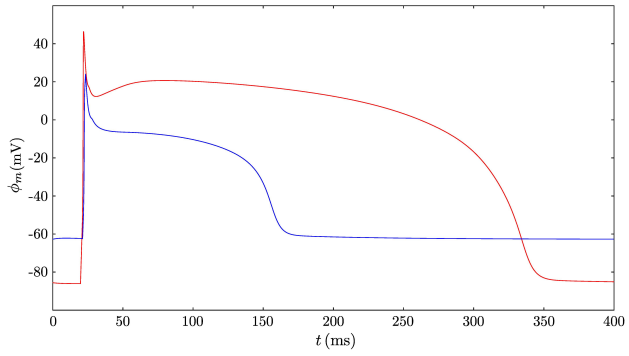

Figure 1. Simulated transmembrane potential over one cardiac cycle for a healthy cell (red) and an ischaemic cell (blue), using the cell model

2.1. Ischaemic geometries

For the rectangular ischaemic geometry, the ischaemic region was defined as the region inside $0° \leq \phi \leq 40°$, $50° \leq \theta \leq 70°$. Three different situations were studied, corresponding to to the ischaemic region extending to 10%, 50% and 90% of the wall thickness.

The cylindrical ischaemic geometry was described as the region given by

$$\frac{(\theta - \theta_m)^2}{a_\theta^2} + \frac{(\phi - \phi_m)^2}{a_\phi^2} \leq 1, \tag{7}$$

where $\theta_m = 60°$, $\phi_m = 20°$, $a_\theta = 10°$ and $a_\phi = 20°$. The same three thickness values used in the rectangular ischaemic geometry were used again for the cylindrical geometry.

The ellipsoidal ischaemic geometry was described as the region given by

$$\frac{r^2}{a_r^2} + \frac{(\theta - \theta_m)^2}{a_\theta^2} + \frac{(\phi - \phi_m)^2}{a_\phi^2} \leq 1, \tag{8}$$

where r represents the perpendicular distance from the centre of the ischaemic region at the endocardium and a_r represents the thickness of the ischaemic region. This was set to $0.1\,cm$, $0.5\,cm$ and $0.9\,cm$, corresponding to the three ischaemic thicknesses. The remaining parameters were the same as described previously.

Smooth border zones were also accounted for in each ischaemic geometry using a similar method as described in [3]. In order for comparison with previously published results [7], the border zones were constructed to be quite sharp, measuring approximately 0.01 cm in width.

2.2. Cell model

The cell model used for the present study, similar to [8], was based on the model described by ten Tusscher and Panfilov [12]. The original model contained a total of 13 transmembrane currents as well as an extensive description of intracellular calcium dynamics. In order to better accommodate ischaemic conditions, an additional ATP activated K^+ current was added to the cell model, using the formulation described by Shaw and Rudy [13]:

$$I_{K,ATP} = \frac{G_{K,ATP}}{1 + \left(\frac{[ATP]_i}{K_{0.5}}\right)^2} \left(\frac{[K^+]_o}{5.4}\right)^{0.24} (\phi_m - E_k),$$

where $G_{K,ATP}$ is the maximum conductance, $[ATP]_i$ is the intracellular ATP concentration, $[K^+]_o$ is the extracellular potassium concentration, E_k is the Nernst equilibrium potential and $K_{0.5}$ the half-maximal saturation point.

2.3. Ischaemic conditions

Ischaemia was modelled at the cellular level by incorporating three of its major physiological consequences.

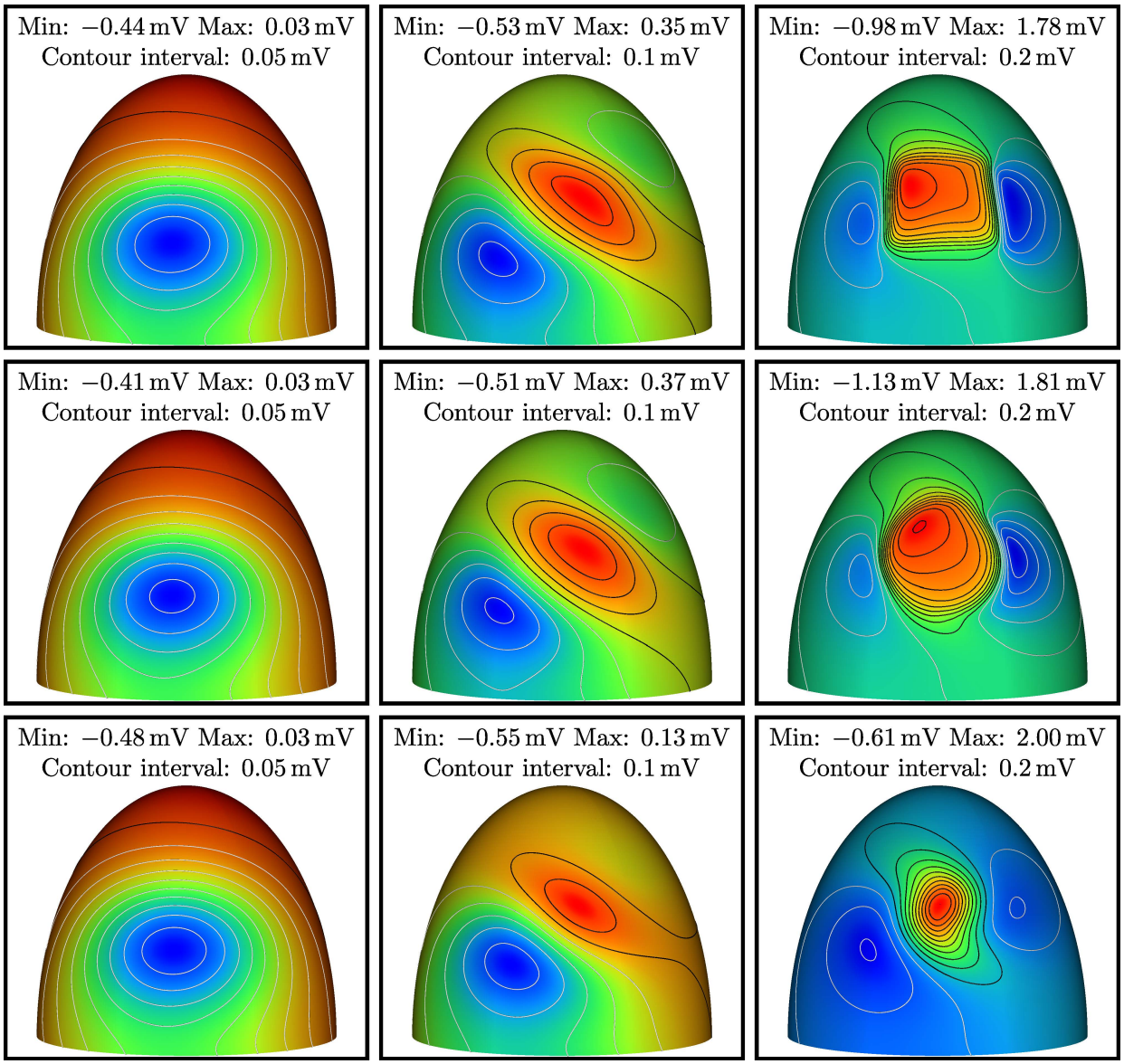

Figure 2. Extracellular epicardial potential distributions at $t = 100$ ms for the rectangular (top row) cylindrical (middle row) and ellipsoidal (bottom row) ischaemic geometries. The columns from left to right correspond to 10%, 50% and 90% ischaemic thickness. Black and white contour lines correspond to positive (including zero) and negative potentials respectively.

1. Hyperkalaemia - Elevated extracellular K^+ concentration, caused by the inability to remove cellular waste and responsible for an increase in resting potential.
2. Acidosis - Affects the fast sodium and L type calcium currents by reducing the conductance of the respective ion channels, resulting in decreased upstroke velocity and plateau potential.
3. Anoxia - Activates the ATP dependent K^+ current, caused by a rise in the extracellular pH levels, resulting in decreased action potential duration.

Hyperkalaemia was achieved by raising $[K^+]_o$ from 5.4 mM to 12 mM. Acidosis was achieved by reducing the conductivity of the fast sodium and L type calcium channels by 25%. Anoxia was simulated by an increase of $K_{0.5}$ from 0.042 to 0.25. Figure 1 shows the transmembrane potential for a single cell using the cell model.

3. Results and discussion

A finite volume method was used to spatially discretise the bidomain equations, and a semi implicit method was

used for the time integration. Parallel code was written in C++ using the PETSc libraries. A timestep of 0.02 ms was used to solve the cell model equations and the PDE's were updated using a timestep of 0.1 ms. At $t = 0$, a stimulus was applied to the model at the apex on the endocardium. A simple Purkinje system was also incorporated by timing the stimulation of the tissue on the endocardium so that the time for the propagation wave to reach the base of the model was 40 ms.

Figure 2 shows the extracellular epicardial potentials obtained from the three different ischaemic geometries for three separate ischaemic thicknesses. For low ischaemic thicknesses, a single depression is visible over the lower edge of the ischaemic region for all three ischaemic geometries. This differs from the observations in the previous slab model studies, where the single depression was located directly over the centre of the ischaemic region. Once the ischaemic region is increased beyond 40%, however, the results become much more interesting, with elevation becoming apparent for the rectangular and cylindrical ischaemic geometries. The results for the ellipsoidal ischaemic geometry differed slightly from the other two at medium thicknesses of ischaemia, with elevation not apparent until the ischaemic thickness increased to approximately 50%. These results are significantly different to those obtained using the slab model, which did not include an elevation for ischaemic thicknesses less than 70%.

At high ischaemic thicknesses ($>$80%), the results looked quite similar to the results from the slab model, with a single elevation apparent over the centre of the ischaemic region.

4. Conclusion

The results presented here show that the rectangular and cylindrical ischaemic geometries give very similar EPDs during the ST segment, while the EPDs from the ellipsoidal ischaemic geometry were slightly different for medium thicknesses of ischaemia. A significant difference was found between the results from the present study and those from the previous studies using a slab model of cardiac tissue. This suggests that the shape of the heart model may also play a large role in determining extracellular potentials as well as the shape of the ischaemic region.

Acknowledgements

We gratefully acknowledge the support of the Griffith University eResearch Services Team and the use of the High Performance Computing Cluster Gowonda to complete this research.

References

[1] Wolferth CC, Bellet S, Livezey MM, Murphy FD. Negative displacement of the rs-t segment in the electrocardiogram and its relationships to positive displacement; an experimental study. American Heart Journal 1945;29(2):220 – 245. ISSN 0002-8703.

[2] Potse M, Coronel R, Falcao S, LeBlanc AR, Vinet A. The effect of lesion size and tissue remodeling on st deviation in partial-thickness ischemia. Heart Rhythm 2007;4(2):200 – 206. ISSN 1547-5271.

[3] Johnston PR. A finite volume method solution for the bidomain equations and their application to modelling cardiac ischaemia. Computer Methods in Biomechanics and Biomedical Engineering 2010;13(2):157–170. ISSN 1025-5842.

[4] MacLeod RS, Shome S, Stinstra J, Punske BB, Hopenfeld B. Mechanisms of ischemia-induced st-segment changes. Journal of Electrocardiology 2005;38(4, Supplement):8 – 13. ISSN 0022-0736.

[5] Holland RP, Brooks H, Lidl B. Spatial and nonspatial influences on the tq-st segment deflection of ischemia: Theoretical and experimental analysis in the pig. The Journal of Clinical Investigation 1977;60(1):197–214.

[6] Li D, Li CY, Yong AC, Kilpatrick D. Source of electrocardiographic st changes in subendocardial ischemia. Circulation Research 1998;82(9):957–970.

[7] Barnes JP, Johnston PR. The effect of the shape of ischaemic regions in the heart on the resulting extracellular epicardial potential distributions. In Computing in Cardiology, 2010, volume 37. ISSN 0276-6547, sept 2010; 177 –180.

[8] Barnes J, Johnston P. The effect of ischaemic region shape on epicardial potential distributions in transient models of cardiac tissue. ANZIAM Journal 2012;53:C110–C126. ISSN 1446-8735.

[9] Tung L. A bi-domain model for describing ischemic myocardial d-c potentials. Ph.D. thesis, Massachusetts Institute of Technology, 1978.

[10] Roth BJ. Action potential propagation in a thick strand of cardiac muscle. Circulation Research 1991;68(1):162–173.

[11] Clerc L. Directional differences of impulse spread in trabecular muscle from mammalian heart. The Journal of Physiology 1976;255(2):335–346.

[12] ten Tusscher KHWJ, Panfilov AV. Alternans and spiral breakup in a human ventricular tissue model. American Journal of Physiology Heart and Circulatory Physiology sep 2006;291(3):H1088–H1100.

[13] Shaw RM, Rudy Y. Electrophysiologic effects of acute myocardial ischemia: a theoretical study of altered cell excitability and action potential duration. Cardiovascular Research 1997;35(2):256–272.

Address for correspondence:

Josef Barnes
School of Biomolecular and Physical Sciences, Griffith University, QLD, Australia
josef.barnes@griffithuni.edu.au